

The impact of spurious imaginary phonon modes on thermal properties of Metal-organic Frameworks

Prathami Divakar Kamath^{1,2}, Kristin A. Persson^{1,2,†}

¹Department of Materials Science & Engineering, University of California, Berkeley, CA, USA

²Materials Sciences Division, Lawrence Berkeley National Laboratory, Berkeley, CA, USA

[†] Corresponding author: kapersson@lbl.gov

Abstract

Metal-organic Frameworks (MOFs) have emerged as potential candidates for direct air capture (DAC) of green house gases and water. Thermal properties of MOFs, such as their heat capacity, are used to determine the energy penalty associated with the adsorbent retrieval during the Temperature Swing Adsorption process. To aid exploration of the vast experimental design space of MOFs for such applications, computational methods like Density Functional Theory (DFT) or surrogate machine learning models trained on DFT data have been developed for obtaining phonon-derived heat capacities of MOFs. However, the high cost of explicit phonon computation in large and flexible nanoporous MOFs often necessitates the use of small supercells or lower convergence criteria which decrease predictive accuracy. These approximations often result in spurious imaginary phonon modes which are commonly ignored in practice. At present, there is no clear consensus in the literature on what magnitude of negative frequency or what fraction of imaginary modes can be considered acceptable. Here, we systematically demonstrate that spurious imaginary phonon modes can introduce substantial errors in heat capacity estimates, leading to incorrect ranking of MOFs in thermal-property-based screening. We further show that benchmarking machine learning interatomic potentials (MLIPs) against DFT datasets containing spurious imaginary modes can misrepresent models that predict physically meaningful phonon spectra for dynamically stable MOFs. Finally, we introduce a simple, rapid post-processing workflow that can be applied to standard phonon calculations to effectively correct heat capacity estimates and account for spurious imaginary modes in MOFs.

Keywords: Imaginary phonon modes, MOFs, Heat capacity, MLIPs, DFT

Introduction

To enable the industrial deployment of Metal-organic frameworks (MOFs)^{1–4} in CO₂ adsorption-based nanotechnologies,^{5–7} heat-management costs during adsorbent regeneration must be considered alongside gas uptake performance.^{8,9} The specific heat capacity of such MOFs¹⁰ directly quantifies the energetic cost of adsorbent recovery in Temperature Swing Adsorption (TSA) processes.¹¹ Accurately computationally predicting this property is therefore critical for realistic screening and design of promising MOFs. This task is complicated by the rich phonon landscape of MOFs,¹² originating from their hybrid organic-inorganic building blocks, flexible linkers, and large unit cells that host hundreds of

vibrational modes. In particular, low-frequency soft phonons drive structural breathing and phase transitions,^{13–16} making phonon-quantized lattice vibrations^{17,18} central to the thermodynamic stability and thermal properties of MOFs.¹⁹

Computationally, phonons are typically calculated within the harmonic approximation²⁰ after a tightly converged structural relaxation, ensuring that atomic forces are effectively zero. In principle, imaginary phonon modes signal true dynamical instabilities, where small atomic perturbations grow exponentially and drive the system toward a lower-energy structure.²¹ In practice, however, spurious imaginary modes are ubiquitous in MOFs, arising from numerical artifacts such as insufficient structural relaxation, inadequate supercell sizes in

finite-difference calculations, and broken translational symmetry.²² The unusually high density of soft vibrational modes in MOFs^{12,23} further amplifies this sensitivity, making the appearance of spurious, imaginary modes dependent on the chosen convergence criteria.

Obtaining high-fidelity phonon spectra for MOFs using density functional theory (DFT)^{24–26} is therefore particularly challenging, as their large unit cells often require supercells containing thousands of atoms.^{27–29} Wieser *et al.*³⁰ showed that near-elimination of imaginary modes is achievable for a small set of well-known MOFs by employing exceptionally tight convergence criteria and large supercells, but at a very high computational cost. While such settings yield highly reliable phonon spectra, they are impractical for large-scale studies involving hundreds of MOFs. Mode mapping and rattling^{22,27,29} can also be employed to eliminate non-physical dynamical instabilities, however, most large-scale phonon datasets rely on looser convergence thresholds and smaller simulation cells. Recent efforts have produced valuable open-access DFT phonon datasets for tens to hundreds of MOFs, notably by Yue *et al.*³¹ and Moosavi *et al.*⁸ Moosavi *et al.*⁸ reported fewer than 2% imaginary modes for most MOFs, while the dataset of Yue *et al.* contained up to 6% imaginary modes. Notably, there is currently no clear consensus on what magnitude of a “small” negative phonon frequency can be considered negligible, with studies adopting different ad hoc cutoffs.^{32–36} In practice, all modes with imaginary frequencies are excluded from thermal property calculations, irrespective of whether their absolute magnitude is as small as 10^{-4} THz or as large as 5 THz.

To extract maximal value from existing MOF phonon datasets, we argue that greater emphasis should be placed on the fraction of spurious imaginary modes that are omitted, rather than on the precise magnitude of their negative frequencies. We show that heat-capacity errors can substantially exceed the percentage of imaginary modes over certain temperature ranges, and that these two quantities cannot be directly equated. Moreover, neglecting imaginary modes can introduce finite errors in heat capacity that lead to underestimated energy penalties and, consequently, to the mis-ranking of MOF candidates. We further caution against using DFT phonon data containing spurious imaginary modes

as reference benchmarks for machine-learning interatomic potentials (MLIPs), as this practice can artificially penalize models that predict physically meaningful phonon spectra. Recognizing the prohibitive computational cost of eliminating spurious imaginary modes with fully converged DFT calculations, we propose a simple post-processing correction for heat-capacity estimation. This approach can be applied in seconds to standard phonon outputs from packages such as Phonopy,³⁷ yielding accuracy comparable to much more expensive calculations. Ultimately, we hope that our work provides guidance for assessing the impact of spurious imaginary modes on heat-capacity calculations and enables users to define application-specific error tolerances.

Results

Effect of Spurious Imaginary Modes on Thermal Properties

In this section, we illustrate the impact of a small fraction of spurious imaginary modes on the thermal properties of MOFs, focusing on two key quantities: the heat capacity and the Debye temperature. The specific heat capacity of MOFs is typically reported in the range of $0.6\text{--}1.4 \text{ Jg}^{-1}\text{K}^{-1}$ at room temperature,³⁸ consistent with the values obtained in our calculations (Table 1). Within the Debye model, the Debye temperature sets the energy scale of the highest acoustic phonon frequencies in a solid and delineates the temperature below which quantum effects in lattice vibrations become significant.¹⁷

As a case study, we use a widely studied and dynamically stable MOF for gas adsorption applications, MOF-74 (with Zinc as the metal node).³⁹ Under the harmonic approximation, the heat capacity with Phonopy³⁷ is estimated with

$$C_v(T) = k_B \sum_i \left(\frac{\hbar\omega_i}{k_B T} \right)^2 \frac{e^{\hbar\omega_i/k_B T}}{(e^{\hbar\omega_i/k_B T} - 1)^2} \quad (1)$$

Current practice often assumes that imaginary frequencies can simply be omitted from Eq. (1); however, each neglected imaginary phonon mode introduces a finite, temperature-dependent error in C_v . As shown in Fig 1 (b), spurious imaginary modes, even as small as 1.03% can lead to an underestimation of C_v by more than 10% in the low temperature region and saturate to errors almost $2\times$ the percentage of imaginary modes at 300 K and higher.

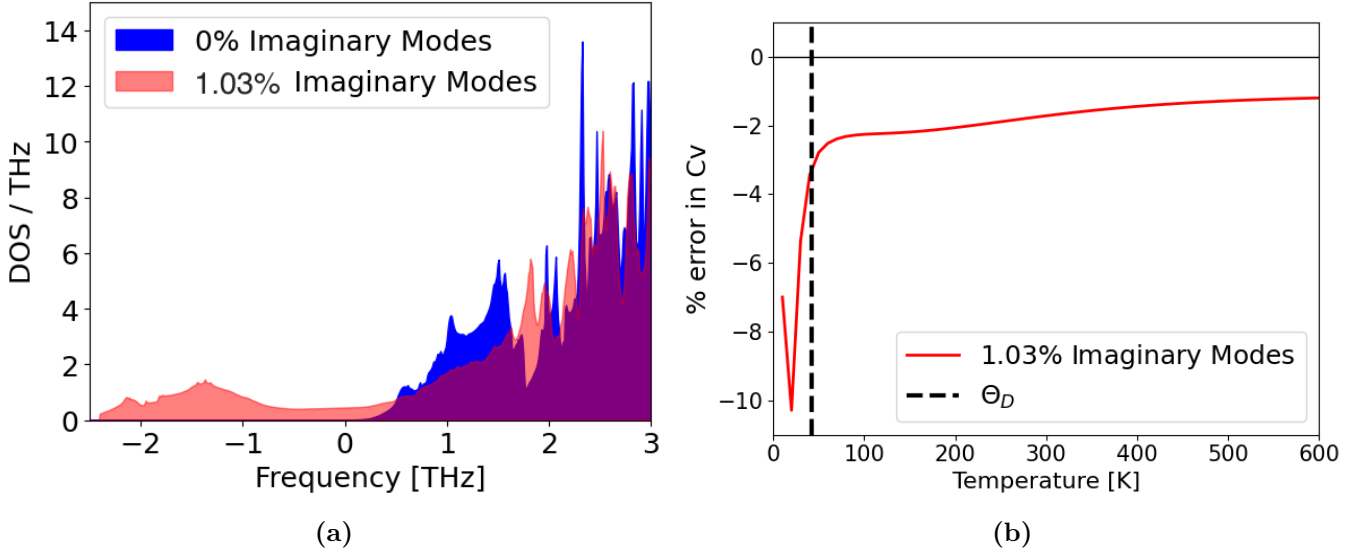


Figure 1: (a) The density of states (DOS) of the two phonon spectra obtained with and without spurious imaginary modes from Moosavi *et al.*⁸ and Wieser³⁰ *et al.* respectively on a $11 \times 11 \times 11$ mesh with the linear tetrahedron approach with a pitch of 0.01 THz. (b) The % deviations in C_v obtained from DFT data with 1.03% spurious imaginary modes relative to 0% shows a strong temperature dependence. θ_D is the proxy Debye temperature of MOF-74 as per equation 3

For complex systems such as MOFs with a large number of phonon branches, the frequency of the lowest optical mode at the Γ -point provides an upper-bound estimate (θ_D) of the true Debye temperature derived from acoustic modes,⁴⁰ as defined in Eq. 3. For MOF-74, this estimate yields $\theta_D \sim 43$ K. In Fig. 1 (b), the abrupt changes observed in the low-temperature regime ($0\text{--}\theta_D$) and the gradual saturation beyond θ_D can be attributed to the nature of the imaginary modes, which correspond to the three acoustic phonon modes and the lowest optical mode branch (see Fig. 2). At temperatures well below θ_D , low-frequency acoustic modes dominate the heat capacity. As shown in Fig. 1(a), these low-frequency modes ($\sim 0\text{--}1$ THz) are absent in the 1.03% imaginary-modes curve. Consequently, the percentage errors in C_v are largest in the $0\text{--}\theta_D$ K range, where the contributions of the imaginary acoustic modes are omitted from the heat capacity calculation. Above θ_D , the percentage errors in C_v gradually decrease as optical phonon modes begin to contribute. Since the number of optical phonon branches scales as $3N - 3$ (where N is the number of atoms in the unit cell, typically > 50 for MOFs), their cumulative contribution rapidly exceeds that of the three acoustic phonons, reducing the impact of neglected imaginary modes on the calculated heat capacity. At $2\theta_D$ and higher tempera-

tures, the average contribution of a mode to $C_v \sim k_b$, reaching the classical Dulong-Petit limit. MOFs generally exhibit a very low Debye temperature owing to their soft and flexible nature as shown in Table 2. For TSA processes, which involve the selective capture of a targeted substance by MOFs at ambient conditions and then release at elevated temperatures, the temperature range of interest is $\gg 2\theta_D$.¹¹ In this temperature range for TSA with MOFs, majority of the low-frequency phonon modes, especially the acoustic modes, can be approximated to be fully active (refer supplementary information (SI) Figure S1 for further details). This explains the constant underestimation in C_v in this temperature range due to the neglected imaginary modes in the calculation.

Owing to the high computational cost of high fidelity DFT calculations, we also report results obtained using MACE-MP-MOF0²⁷ in Table 1. MACE-MP-MOF0 is a fine-tuned machine-learning interatomic potential (MLIP) designed for high-throughput phonon calculations of MOFs, for which tight convergence criteria can be readily applied to eliminate spurious imaginary modes. Given the excellent agreement between the specific heat capacity predictions from MACE-MP-MOF0 and DFT, this model is used as a surrogate for the 0% imaginary-mode DFT baseline to extend the analysis to a broader and more diverse set of MOFs beyond MOF-

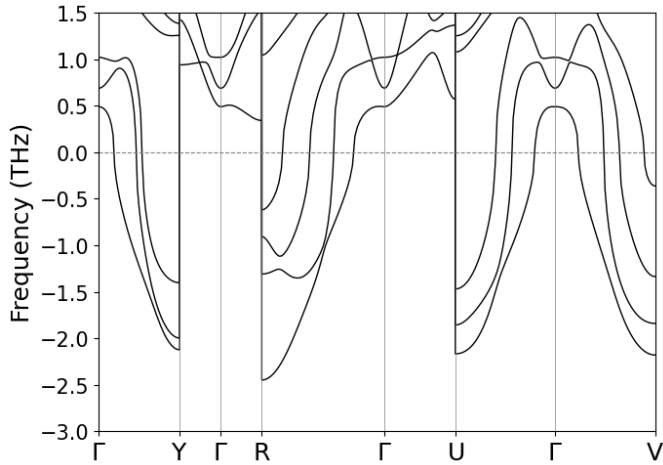


Figure 2: The phonon band diagram for MOF-74 obtained from the force constants reported in Moosavi *et al.*⁸ using the primitive unit cell and relatively loose convergence criteria produces imaginary phonon modes for the branches corresponding to 3 acoustic and the lowest optical phonon mode.

74.

Table 1 shows that, even when MLIPs reproduce DFT phonon properties with high fidelity, comparisons with experiment remain uncertain due to intrinsic DFT errors and the 1–3% variability reported for the specific heat capacity of the same MOF across careful differential scanning calorimetry measurements.¹⁰ For two distinct MOFs that often differ by only \sim 1–2% in C_v , errors arising from spurious imaginary modes can match or exceed these uncertainties, thereby risking mis-ranking of MOF performance due to convergence criteria rather than fundamental limitations of DFT or MLIPs.

Hence, we propose a simple fix to account for the missing spurious imaginary modes by adding a correction term to the $C_v(T)_{\text{imaginary}}$ output from phonopy for $T > 2\theta_D$ given by equation 2.

$$C_v(T)_{\text{corrected}} = C_v(T)_{\text{imaginary}} + k_B T \left(3N \frac{\% \text{ imaginary_modes}}{100} \right) \quad (2)$$

By assuming a full k_b contribution at $T \sim 2\theta_D$ from the imaginary optical mode, this approach introduces a modest overestimation comparable in magnitude to the uncorrected data shown in Fig. 3(a). However, it also reduces the percentage error in C_v from 1.7% to 0.23% - nearly an order of magnitude - at 300 K and higher temperatures within our range of interest, resulting in an excellent agreement in Fig. 3(b). Thus, rather than simply omitting imaginary modes, this inexpensive post-processing

correction can be readily applied and yields near-quantitative agreement with imaginary mode-free DFT results at moderate and high temperatures.

Systematic dependence of C_v errors on % Imaginary Modes

In order to quantify the extent to which fraction of imaginary modes affect heat capacity predictions and to demonstrate the generalization of the proposed post-processing method across a diverse group of five MOFs, we investigate DFT phonon and C_v data from Yue *et al.*³¹ (See Methods Section for details on the chosen MOFs). Using MACE-MP-MOF0 as a substitute for DFT for the 0% imaginary mode baseline, Fig 4 shows that DFT data with spurious imaginary modes varying from 0.71% to 5.75% leads to underestimations in C_v at 300K from -1.5% to -12.2% respectively. This data indicates that the error in C_v at 300K is more than 2 times the observed percentage of imaginary modes. Hence, for heat-capacity predictions of MOFs, maintaining spurious imaginary modes below a threshold of 0.5% limits errors in C_v to under 1%, enabling reliable discrimination between distinct MOFs (as discussed in the previous section) without requiring post-processing corrections.

After adding the corrected contribution as per equation 2 to the imaginary-mode DFT data, the percentage errors in C_v decrease by an order of magnitude across all five examples demonstrating the robustness of the approach. Importantly, none of the

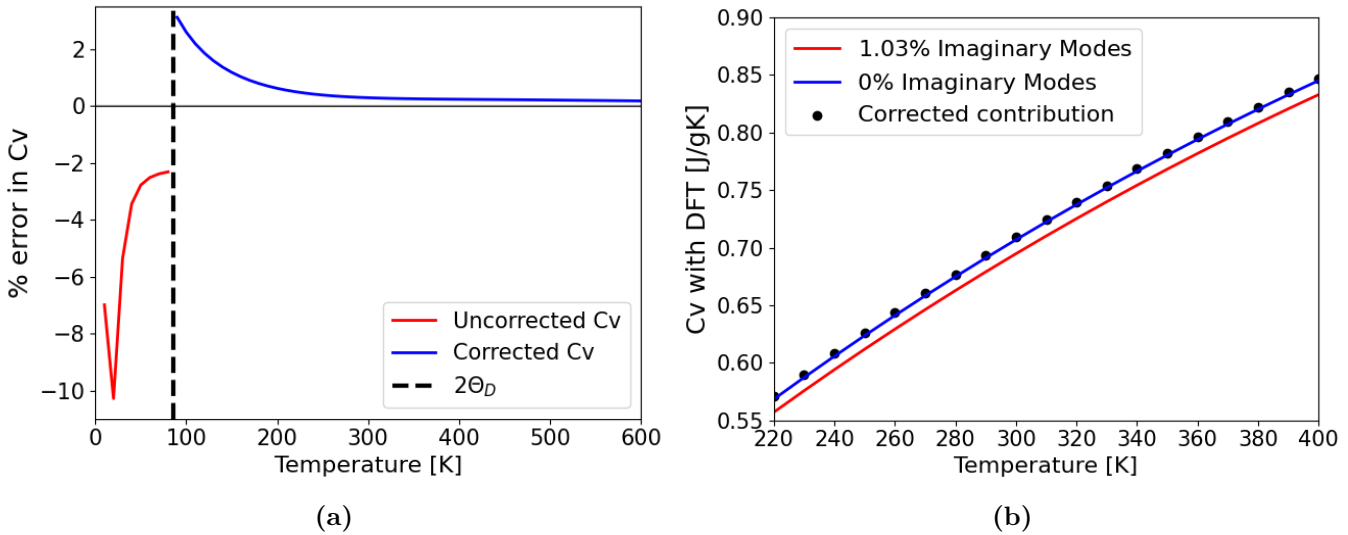


Figure 3: (a) The % deviations in C_v obtained from DFT data with 1.03% spurious imaginary modes relative to 0% become significantly lower at $T \gg \theta_D$ after adding corrections (b) A constant underestimation $\sim 2\%$ can be seen in C_v at temperatures around 300K due to the imaginary modes in the red curve. Accounting for the imaginary modes in the corrected contribution curve leads to a nearly perfect overlap with the blue 0% Imaginary Modes Curve.

MOF	Experimental C_p	DFT C_v	MACE-MP-MOF0 C_v	MACE-MP-MOF0 C_p
Zn-MOF-5	0.77 ⁴¹	0.79	0.79	0.79
Zr-UiO-66	0.78 ⁴²	0.78	0.78	0.78
Zn-MOF-74	0.66 ⁸	0.71	0.71	0.71
Al-MIL-53	0.86 ⁴¹	1.01	1.01	1.01

Table 1: Constant pressure and volume specific heat capacity predictions (C_p and C_v respectively in $Jg^{-1}K^{-1}$) at room temperature. C_p data with MACE-MP-MOF0 is obtained under the quasi-harmonic approximation. The DFT C_v data was computed using the force constants from³⁰ as a reliable reference since there were $\sim 0\%$ imaginary modes. Refer the Methods Section for more details

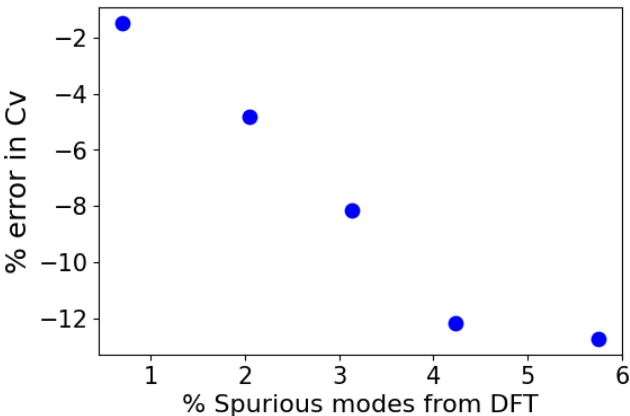
selected MOFs were included in the training of the MACE-MP-MOF0 model. Therefore, the remaining errors after applying corrections to the DFT data may partially reflect the intrinsic accuracy of the model. Nevertheless, all deviations remain small, within an absolute error of 0.8%

Comparisons of DFT data with MLIP in the ranking of MOF Heat Capacity

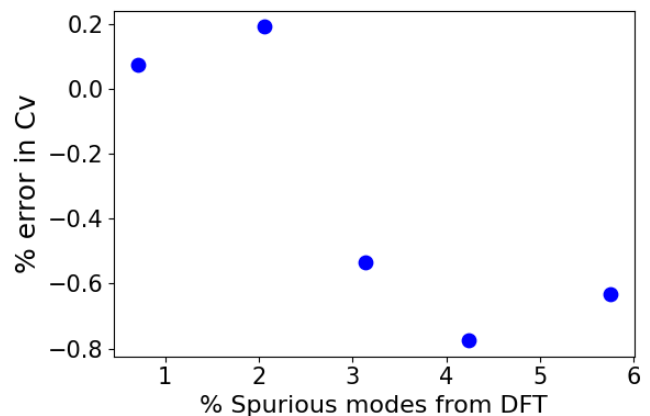
The rapidly expanding development of universal and fine-tuned MLIPs for MOFs has prompted increased efforts to benchmark their performance in predicting MOF physical properties. The analysis in the previous subsection suggests that even small spurious imaginary modes in DFT can artificially re-rank the heat capacities of MOFs relative to MLIP predictions with 0% imaginary modes, potentially leading

to the incorrect conclusion that an MLIP performs poorly. One recent example is MOFSimBench,⁴³ which compares the performance of 20 MLIPs in predicting MOF heat capacities relative to DFT reference data from Moosavi *et al.*,⁸ which contain $\sim 2\%$ imaginary modes. The authors report a systematic overestimation of C_v by MLIPs relative to DFT, attributing this behavior to softening of the potential energy surface in MLIPs - a phenomenon also observed in other studies.⁴⁴

We hypothesize that, in addition to this effect, a substantial contribution to the apparent MLIP overestimation arises from the presence of spurious imaginary modes in the reference DFT data, which are neglected in the heat capacity calculations. To test this hypothesis, we examine MOF-74 using MACE-MP-MOF0, which was identified



(a)



(b)

Figure 4: (a) The deviations (%) in C_v obtained from DFT data with increasing spurious imaginary modes in different MOFs relative to the 0% imaginary-modes data from MACE-MP-MOF0. (b) The deviations (%) in the corrected C_v obtained from post-processing the DFT data are $10\times$ smaller for all MOFs relative to the 0% imaginary-modes data from MACE-MP-MOF0.

as one of the top-performing models in MOFSimBench,⁴³ with a reported mean percentage absolute error (MPAE) of 2.5% relative to DFT. As shown in Fig. 5, MACE-MP-MOF0 overestimates C_v by 2.53% in agreement with the reported MPAE when benchmarked against the same DFT reference data containing 1.03% imaginary modes used in MOFSimBench.⁴³ In contrast, when using DFT data with 0% imaginary modes from Wieser *et al.*,³⁰ as well as the corrected DFT data introduced in this work, the apparent overestimation by MACE-MP-MOF0 is substantially reduced to 0.77%. The MOFSimBench⁴³ study does not report whether imaginary modes were present and then neglected in the computation of C_v across the 20 MLIPs considered, making it difficult to determine whether the observed overestimation reflect true model accuracy or compensating effects from imaginary modes in the MLIPs. (Refer SI Figure S4 (c) for an example).

While benchmarking MLIP performance or identifying best-performing models is not the primary focus of this work, we present an illustrative example demonstrating how models containing spurious imaginary modes can appear to exhibit lower errors when benchmarked against insufficiently converged DFT reference data. To this end, we compare MACE-MP-MOF0 with another recently fine-tuned MLIP for phonon and heat capacity prediction in MOFs proposed by Yue *et al.*³¹ using the reported DFT reference data in that study. We analyze two Zn-based MOFs from the previous sec-

tion drawn from the QMOF database,^{45,46} which exhibit 5.75% (ID “qmof-08b5558”) and 2.06% (ID “qmof-574737f”) spurious imaginary modes in the DFT phonon spectra. For the MOF “qmof-08b5558” shown in Fig. 6(a), the Yue *et al.*³¹ (referred to as **MLP** in both their work and ours), **MLP** predicts 4.97% imaginary modes, whereas MACE-MP-MOF0 yields zero imaginary modes. If the reference DFT data are used without correcting for spurious imaginary modes in the C_v calculation, MACE-MP-MOF0 would be characterized as the inferior model, exhibiting an apparent deviation of $\sim 12.7\%$ at 300 K. In contrast, when the post-processed DFT C_v data is used, MACE-MP-MOF0 achieves near-quantitative agreement with a deviation of 0.5%, while the Yue *et al.*³¹ **MLP** shows a $\sim 10\times$ larger deviation of 6.5% relative to the corrected DFT reference. For the MOF “qmof-574737f” shown in Fig. 6(b), where the Yue *et al.*³¹ **MLP** also predicts $\sim 0\%$ imaginary modes, both MLIPs show improved agreement with the post-processed DFT C_v data, with errors of $\sim 0.18\%$ at 300 K. These results underscore the importance of accounting for spurious imaginary modes in benchmarking analyses, as avoidable, model- and reference-data-specific errors can otherwise bias screening and ranking outcomes.

Discussion

This work systematically elucidates the impact of spurious imaginary phonon modes arising from com-

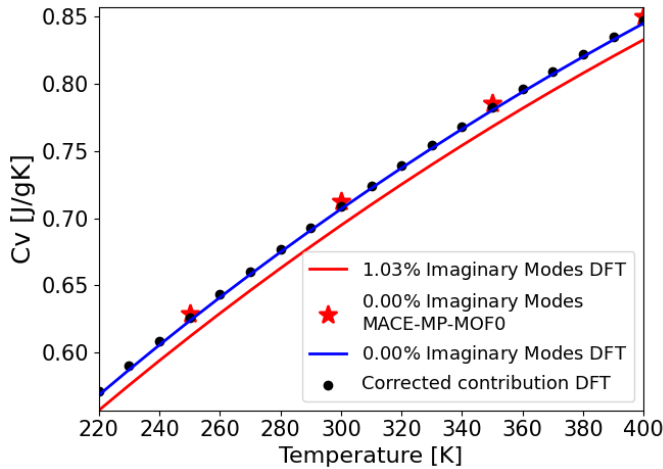


Figure 5: The C_v curve from DFT data containing 1.03% spurious imaginary modes shows a constant underestimation relative to other DFT³⁰ and MACE-MP-MOFO data containing $\sim 0\%$ imaginary modes. The corrected contribution to the DFT data bridges this gap

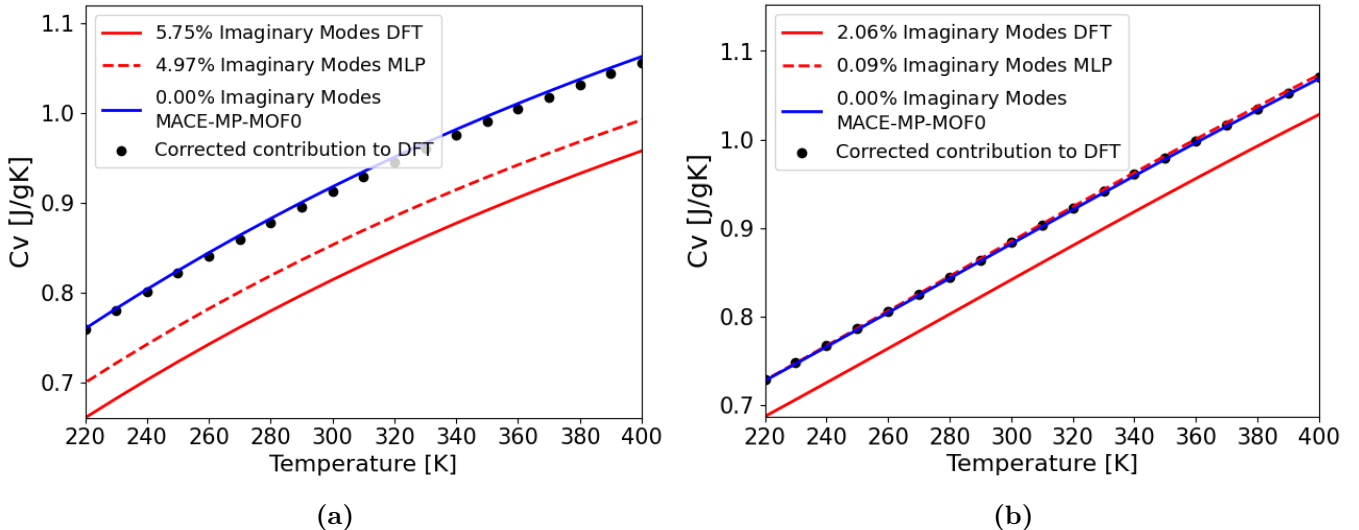


Figure 6: The C_v curves obtained from DFT with and without corrections for imaginary modes compared against MACE-MP-MOFO and the MLP from Yue *et al.*³¹ for (a) "qmof-08b5558" and (b) "qmof-574737f"

mon computational approximations, such as insufficient structural relaxation, inadequate supercell sizes in finite-difference calculations, and broken translational symmetry — issues that are particularly prevalent in MOFs due to their large unit cells and computationally demanding relaxations. Although such imaginary modes are generally regarded as artifacts, their contributions are often neglected without a systematic assessment of their influence on calculated thermal properties.

Rather than prescribing a single universally “correct” threshold for acceptable imaginary modes in phonon calculations, we present an analysis that

quantifies the consequences of specific methodological choices on the physical properties of MOFs, enabling users to assess the impact on their intended applications and make informed decisions about how to treat observed imaginary modes. With accurate, imaginary mode-free phonons - or with strategies to eliminate spurious imaginary modes that are more readily achievable using modern MLIPs due to their computational efficiency - we argue that MLIP benchmarking should go beyond property-level agreement and explicitly verify the physical validity of the underlying phonon spectra. This distinction between spurious imaginary modes and gen-

uine dynamical instabilities is essential for obtaining reliable derived properties and for overcoming the scalability limitations of DFT. When fully imaginary mode-free DFT phonon data for MOFs are not feasible, the proposed post-processing workflow provides an efficient and practical alternative for benchmarking MLIPs against DFT. The accompanying code is publicly available on GitHub and requires only standard Phonopy output files as input, enabling improved accuracy with negligible additional computational effort.

Ultimately, this work demonstrates how approximations at the nanoscale vibrational level propagate to macroscopic thermophysical properties. Neglecting spurious imaginary phonon modes leads to systematic underestimation of heat capacity, which in turn results in a comparable underprediction of the energy required for MOF regeneration in CO₂ temperature swing adsorption processes. Such errors can distort materials screening and ranking, causing some candidates to appear more efficient than they truly are.

Methods

Phonon and Heat Capacity Computations

The DFT force constants used to compute heat capacities in this work which were taken from Moosavi *et al.*,⁸ Yue *et al.*,³¹ and Wieser *et al.*³⁰ were all computed using the PBE+ D3(BJ)^{47–49} functional and the trained MLIPs, MACE-MP-MOF0²⁷ and the **MLP** from Yue *et al.*³¹ were also trained on datasets generated with the same DFT functional ensuring consistency in our comparisons. The constant volume heat capacity C_v data reported in this study was computed under the harmonic approximation with the Phonopy³⁷ package, using the force constants on a $11 \times 11 \times 11$ mesh for temperatures from 0 to 1000K. The % spurious modes are computed from the number of modes neglected in the thermal properties calculation with cutoff frequency set to zero.

Among the thermal properties included in the standard output of Phonopy which are the vibrational Helmholtz free energy (F), Entropy (S) and Energy (U) in addition to Heat Capacity (C_v), C_v has been the main focus here since it is a more directly measurable property reported in experimental literature for MOFs. This allows us to correlate the impact of computational artifacts like spurious imag-

inary modes to real-world applications such as energy penalty estimations from heat capacity. But to understand how the error in C_v from spurious imaginary modes propagates through other derived thermodynamic variables, refer the SI Figure S5. In order to compare experimental C_p , the quasi-harmonic approximation²⁰ was used to introduce the volume dependence indirectly with harmonic computations at $\pm 3\%$ linear strain for seven configurations around the equilibrium volume. Because of the expensive nature of this approximation with DFT for MOFs, we generated C_p data only with MACE-MP-MOF0. The negligible difference seen between C_p and C_v in Table 1 allows for more large scale analysis of the heat capacity of MOFs as the significantly cheaper harmonic phonon approximation can be used.

The harmonic phonon computations with MACE-MP-MOF0 were performed by starting with a tight structural relaxation until the maximum force on the atoms is 10^{-8} eV/Å and creating a supercell with minimum 20Å length to capture long-range interactions for the finite difference approach. The density of states and thermal properties were computed with the aforementioned mesh. None of the resultant phonon spectra from MACE-MP-MOF0 for the MOFs considered in this study needed elimination of any spurious imaginary modes.

Chosen MLIPs and MOFs for the benchmarking example

The MACE-MP-MOF0 and Yue *et al.* **MLP**³¹ were chosen to demonstrate an example of benchmarking as both models included training datasets spanning several equilibrium and out-of-equilibrium configurations of MOFs and have been previously studied for their phonon performance. While MACE-MP-MOF0 covers different metal-node based MOFs, since the other model only covers zinc (Zn) metal nodes, the chosen MOFs are Zn-based with diverse linkers and topologies to be compatible with both models as summarized in Table 2. Furthermore, to consider a wide range of % imaginary modes for systematic evaluation, phonon spectra for all 40 MOFs sampled by Yue *et al.*³¹ from the QM0F database^{45,46} were analyzed to select five unique % values as shown in Table 2.

QMOF ID	LCD (Å)	No. of atoms	Spacegroup	θ_D (K) from MACE-MP-MOF0	% imaginary modes from DFT ³¹
qmof-f75eb5a	6.09773	34	Cc	72.76	0.71
qmof-574737f	5.10389	38	Cc	37.57	2.06
qmof-b12c68c	1.79097	40	P-1	88.97	3.13
qmof-fab2f1a	3.82654	43	C2/m	61.79	4.24
qmof-08b5558	2.11616	39	<i>P</i> 3 ₁ 21	84.73	5.75

Table 2: The key characteristics of the five MOFs sampled from the QMOF database^{45,46} that were studied in Yue *et al.*³¹ along with their proxy estimates for the Debye Temperature. Refer SI Figure S2 for the structural details of these MOFs

Estimation of the Debye Temperature

The phonon spectra of MOFs are characterized by several low frequency acoustic and optical phonon modes due to their soft and flexible nature as shown in the phonon band diagrams of MOF-74 in Figure 2 and the five MOFs considered in this study (refer SI Figure S3). The lowest optical mode frequency at the Γ point ($\omega_{\text{opt}}^{\text{min}}$) serves a quick proxy and upper limit to the Debye cutoff frequency (ω_D) of the acoustic phonons.⁴⁰ This provides a rough estimation of the Debye temperature (θ_D) for framework structure according to the equation

$$\theta_D = \frac{\hbar\omega_D}{k_b} \sim \frac{\hbar\omega(\Gamma)^{\text{min}}}{k_b} \quad (3)$$

Table 2 summarizes the θ_D estimates from MACE-MP-MOF0 with $\sim 0\%$ imaginary modes for several MOFs to provide an idea about the range of Debye temperatures of MOFs and that the corrected contribution can be safely applied at 300K and higher temperatures. This proxy is used rather than a rigorous estimation of the Debye temperature as the purpose of this computation is to show that the room temperature and higher ranges are far greater than the range of θ_D for MOFs. In cases where the phonon band diagrams contain spurious imaginary modes, θ_D should not be estimated directly as the acoustic phonon branches would be shifted below the 0 THz frequency limit which can lead to nonphysical predictions of temperatures.

Data Availability Statement

The code for the proposed solution as well as the DFT and MLIP outputs have been made available on Github https://github.com/prathami11/Spurious_ImaginaryModes/tree/main

Acknowledgments

This research used resources of the National Energy Research Scientific Computing Center (NERSC), a Department of Energy Office of Science User Facility. PDK acknowledges financial support from U.S. National Science Foundation's "The Quantum Sensing Challenges for Transformational Advances in Quantum Systems (QuSeC-TAQS)" program.

Author Contribution

All authors contributed towards the conceptualization of the work. PDK led the investigation, generated all the data for the results reported and drafted the manuscript. KAP supervised the research and guided data interpretation and assisted with drafting the manuscript.

Supplementary Information

Supplementary data is uploaded as an ancillary file accompanying this article.

References

- [1] Zhou H.-C., Long J. R., and Yaghi O. M. Introduction to metal-organic frameworks. *Chem. Rev.*, 112:673–674, 2012.
- [2] Hiroyasu Furukawa, Kyle E. Cordova, Michael O’Keeffe, and Omar M. Yaghi. The chemistry and applications of metal-organic frameworks. *Science*, 341(6149):1230444, 2013.
- [3] Omar M. Yaghi, Michael O’Keeffe, Nathan W. Ockwig, Hee K. Chae, Mohamed Eddaoudi, and Jaheon Kim. Reticular synthesis and the design

of new materials. *Nature*, 423(6941):705–714, 2003.

[4] Hailian Li, Mohamed Eddaoudi, M. O’Keeffe, and O. M. Yaghi. Design and synthesis of an exceptionally stable and highly porous metal-organic framework. *Nature*, 402(6759):276–279, 1999.

[5] Anuroop Sriram, Sihoon Choi, Xiaohan Yu, Logan M. Brabson, Abhishek Das, Zachary Ulissi, Matt Uyttendaele, Andrew J. Medford, and David S. Sholl. The open dac 2023 dataset and challenges for sorbent discovery in direct air capture. *ACS Central Science*, 10(5):923–941, 05 2024.

[6] H. H. Do, I. Rabani, and H. B. Truong. Metal-organic framework-based nanomaterials for co₂ storage: A review. *Beilstein Journal of Nanotechnology*, 14:964–970, September 2023.

[7] Shreya Mahajan and Manu Lahtinen. Recent progress in metal-organic frameworks (mofs) for co₂ capture at different pressures. *Journal of Environmental Chemical Engineering*, 10(6):108930, 2022.

[8] Seyed Mohamad Moosavi, Bohumil A. Novotny, Daniele Ongari, Elie Moubarak, Morteza Asgari, Özgür Kadioglu, Constantinos Charalambous, Antonio Ortega-Guerrero, Amir H. Farmahini, Lev Sarkisov, Sergio Garcia, Frank Noé, and Berend Smit. A data-science approach to predict the heat capacity of nanoporous materials. *Nature Materials*, 21(12):1419–1425, December 2022.

[9] Jelle Wieme, Steven Vandenbrande, Aran Lamaire, Venkat Kapil, Louis Vanduyfhuys, and Veronique Van Speybroeck. Thermal engineering of metal-organic frameworks for adsorption applications: A molecular simulation perspective. *ACS Applied Materials & Interfaces*, 11(42):38697–38707, 10 2019.

[10] S. Rudtsch. Uncertainty of heat capacity measurements with differential scanning calorimeters. *Thermochimica Acta*, 382(1):17–25, 2002. Developments in Calorimetry 2001.

[11] Jarad A. Mason, Kenji Sumida, Zoey R. Herm, Rajamani Krishna, and Jeffrey. R. Long. Evaluating metal-organic frameworks for post-combustion carbon dioxide capture via temperature swing adsorption. *Energy Environ. Sci.*, 4:3030–3040, 2011.

[12] Anastasia B. Andreeva, Khoa N. Le, Lihaokun Chen, Michael E. Kellman, Christopher H. Hendon, and Carl K. Brozek. Soft mode metal-linker dynamics in carboxylate mofs evidenced by variable-temperature infrared spectroscopy. *Journal of the American Chemical Society*, 142(45):19291–19299, 11 2020.

[13] Cockayne E. Thermodynamics of the flexible metal-organic framework material mil-53(cr) from first principles. *J. Phys. Chem. C*, 121:4312–4317, 2017.

[14] M. Alhamami, H. Doan, and C. H. Cheng. A review on breathing behaviors of metal-organic-frameworks (mofs) for gas adsorption. *Materials (Basel)*, 7(4):3198–3250, April 2014.

[15] Alexander E. J. Hoffman, Irena Senkovska, Leila Abylgazina, Volodymyr Bon, Veronika Grzimek, Anna Maria Dominic, Margarita Russina, Marvin A. Kraft, Inez Weidinger, Wolfgang G. Zeier, Veronique Van Speybroeck, and Stefan Kaskel. The role of phonons in switchable mofs: a model material perspective. *J. Mater. Chem. A*, 11:15286–15300, 2023.

[16] Filip Formalik, Michael Fischer, and Bogdan Kuchta. Correlating phonons and deformations: A method for structural phase transformation analysis in metal-organic frameworks. *Crystal Growth & Design*, 23(12):8962–8971, 12 2023.

[17] Bogdan Kuchta, Filip Formalik, Justyna Rogacka, Alexander V. Neimark, and Lucyna Firlej. Phonons in deformable microporous crystalline solids. *Zeitschrift für Kristallographie - Crystalline Materials*, 234(7-8):513–527, 2019.

[18] J. M. Ziman. *Electrons and Phonons: The Theory of Transport Phenomena in Solids*, volume 540. Oxford University Press, 2001.

[19] Sandro Wieser, Tomas Kamencek, Johannes P. Dürholt, Rochus Schmid, Natalia Bedoya-Martínez, and Egbert Zojer. Identifying the bottleneck for heat transport in metal-organic frameworks. *Advanced Theory and Simulations*, 4(1):2000211, 2021.

[20] Mason T. Agne, Shashwat Anand, and G. Jeffrey Snyder. Inherent anharmonicity of harmonic solids. *Research*, 2022:9786705, 2022.

[21] Niraj K. Nepal, Paul C. Canfield, and Lin-Lin Wang. Imaginary phonon modes and phonon-mediated superconductivity in y_2c_3 . *Phys. Rev. B*, 109:054518, Feb 2024.

[22] Ioanna Pallikara, Prakriti Kayastha, Jonathan M Skelton, and Lucy D Whalley. The physical significance of imaginary phonon modes in crystals. *Electronic Structure*, 4(3):033002, jul 2022.

[23] Christopher M. Owen and Michael J. Lawler. Generic rigidity and accidental modes in metal-organic frameworks, 2025.

[24] W. Kohn, A. D. Becke, and R. G. Parr. Density functional theory of electronic structure. *The Journal of Physical Chemistry*, 100(31):12974–12980, 01 1996.

[25] P. Hohenberg and W. Kohn. Inhomogeneous electron gas. *Phys. Rev.*, 136:B864–B871, Nov 1964.

[26] Reiner M. Dreizler and Eberhard K. U. Gross. *Density Functional Theory: An Approach to the Quantum Many-Body Problem*. Springer Book Archive. Springer-Verlag Berlin Heidelberg, Berlin, Heidelberg, 1 edition, 1990. Published: 06 December 2012.

[27] Elena A. M., Kamath P. D., Jaffrelot Inizan T., Rosen A. S., Zanca F., and Persson K. A. Machine learned potential for high-throughput phonon calculations of metal-organic frameworks. *npj Comput. Mater.*, 11:125, 2025.

[28] Tomas Kamencuk, Sandro Wieser, Hirotaka Kojima, Natalia Bedoya-Martínez, Johannes P. Dürholt, Rochus Schmid, and Egbert Zojer. Evaluating computational shortcuts in supercell-based phonon calculations of molecular crystals: The instructive case of naphthalene. *Journal of Chemical Theory and Computation*, 16(4):2716–2735, 04 2020.

[29] Jessica K. Bristow, Jonathan M. Skelton, Katrine L. Svane, Aron Walsh, and Julian D. Gale. A general forcefield for accurate phonon properties of metal-organic frameworks. *Phys. Chem. Chem. Phys.*, 18:29316–29329, 2016.

[30] Wieser S. and Zojer E. Machine learned force-fields for an ab-initio quality description of metal-organic frameworks. *npj Comput. Mater.*, 10:18, 2024.

[31] Yifei Yue, Saad Aldin Mohamed, N. Duane Loh, and Jianwen Jiang. Toward a generalizable machine-learned potential for metal-organic frameworks. *ACS Nano*, 19(1):933–949, 01 2025.

[32] Takuya Naruse, Atsuto Seko, and Isao Tanaka. A systematic approach to crystal structure prediction following imaginary phonon modes combined with polynomial machine learning potentials. *Journal of the Physical Society of Japan*, 94(7):074601, 2025.

[33] Rebecca Sure and Stefan Grimme. Comprehensive benchmark of association (free) energies of realistic host–guest complexes. *Journal of Chemical Theory and Computation*, 11(8):3785–3801, 08 2015.

[34] Ze-Hua Wang, Meng-Yao Dai, Hua-Biao Yu, Yi-Neng Huang, Li-Li Zhang, and Bo-Cheng Lei. First-principles study of the sc2cf2/ws2 heterostructure: Electronic structure and strain effects. *Journal of Applied Physics*, 138(24):244301, 12 2025.

[35] Tunable ferroelectricity in oxygen-deficient perovskites with grenier structure. *npj Computational Materials*, 9(1):218, 2023.

[36] Vei Wang, Gang Tang, Ya-Chao Liu, Ren-Tao Wang, Hiroshi Mizuseki, Yoshiyuki Kawazoe, Jun Nara, and Wen Tong Geng. High-throughput computational screening of two-dimensional semiconductors. *The Journal of Physical Chemistry Letters*, 13(50):11581–11594, 12 2022.

[37] Atsushi Togo and Isao Tanaka. First principles phonon calculations in materials science. *Scripta Materialia*, 108:1–5, 2015.

[38] Bin Mu and Krista S. Walton. Thermal analysis and heat capacity study of metal-organic

frameworks. *The Journal of Physical Chemistry C*, 115(46):22748–22754, 11 2011.

[39] Dipak Adhikari, Ravi Karki, Kapil Adhikari, and Nurapati Pantha. In silico study of co, co₂, and ch₄ adsorption on m-mof-74 (m = mg, zn, cu). *ACS Omega*, 10(43):51205–51214, 11 2025.

[40] Aimei Zhou, Denan Li, Mingshu Tan, Yanpei Lv, Simin Pang, Xinxing Zhao, Zhifu Shi, Jun Zhang, Feng Jin, Shi Liu, and Lei Sun. Phononic modulation of spin-lattice relaxation in molecular qubit frameworks. *Nature Communications*, 15(1):10763, 2024.

[41] F.A. Kloutse, R. Zacharia, D. Cossement, and R. Chahine. Specific heat capacities of mof-5, cu-btc, fe-btc, mof-177 and mil-53 (al) over wide temperature ranges: Measurements and application of empirical group contribution method. *Microporous and Mesoporous Materials*, 217:1–5, 2015.

[42] Hoa Thi Lai, Nhat Quang Minh Tran, Linh Ho Thuy Nguyen, Thu Bao Nguyen Le, Cuong Chi Nguyen, Anh Tuan Thanh Pham, Tan Le Hoang Doan, Sungkyun Park, Jongill Hong, Gerald Jeffrey Snyder, and Thang Bach Phan. Low experimental thermal conductivity of zirconium metal-organic framework uiq-66. *Applied Physics Letters*, 124(15):152205, 04 2024.

[43] Kraß H., Huang J., and Moosavi S. M. Mofsim-bench: Evaluating universal machine learning interatomic potentials in metal-organic framework molecular modeling. *arXiv preprint*, arXiv:2507.11806, 2025.

[44] Bowen Deng, Yunyeong Choi, Peichen Zhong, Janosh Riebesell, Shashwat Anand, Zhuohan Li, KyuJung Jun, Kristin A. Persson, and Gerbrand Ceder. Systematic softening in universal machine learning interatomic potentials. *npj Computational Materials*, 11(1):9, 2025.

[45] Rosen A. S., Iyer S. M., Ray D., Yao Z., Aspuru-Guzik A., Gagliardi L., Notestein J. M., and Snurr R. Q. Machine learning the quantum-chemical properties of metal-organic frameworks for accelerated materials discovery. *Matter*, 4:1578–1597, 2021.

[46] Rosen A. S., Fung V., Huck P., O'Donnell C. T., Horton M. K., Truhlar D. G., Persson K. A., Notestein J. M., and Snurr R. Q. High-throughput predictions of metal-organic framework electronic properties: theoretical challenges, graph neural networks, and data exploration. *npj Comput. Mater.*, 8:112, 2022.

[47] Perdew J. P., Burke K., and Ernzerhof M. Generalized gradient approximation made simple. *Phys. Rev. Lett.*, 77:3865–3868, 1996.

[48] Grimme S., Antony J., Ehrlich S., and Krieg H. A consistent and accurate ab initio parametrization of density functional dispersion correction (dft-d) for the 94 elements h–pu. *J. Chem. Phys.*, 132:154104, 2010.

[49] Grimme S., Ehrlich S., and Goerigk L. Effect of the damping function in dispersion corrected density functional theory. *J. Comput. Chem.*, 32:1456–1465, 2011.